Hingst Mary (Orcid ID: 0000-0003-3600-003X)
McQuiggan Rachel (Orcid ID: 0000-0002-3609-071X)

Research Paper

Surface water-groundwater connections as pathways for inland salinization of coastal aquifers

Mary C. Hingst
University of Delaware Department of Earth Sciences, Newark, DE, USA; hingstma@udel.edu

Rachel W. McQuiggan
Delaware Geological Survey, Newark, DE, USA; rmcquiggan@udel.edu

Chelsea N. Peters
Roanoke College Department of Environmental Studies; peters@roanoke.edu

Changming He
Delaware Geological Survey, Newark, DE, USA; hchm@udel.edu

A. Scott Andres
Delaware Geological Survey, Newark, DE, USA; asandres@udel.edu

Holly A. Michael
University of Delaware Department of Earth Sciences and Department of Civil and Environmental Engineering, Newark, DE, USA; hmichael@udel.edu

Corresponding author: Holly A. Michael

Conflict of Interest: None.

Key words: salinization, saltwater intrusion, coastal groundwater, tidal streams, agriculture, irrigation

Article Impact Statement (137/140-character limit): *Expedited salinization of aquifers via surface water-groundwater connections poses risks to coastal wells near marshes and tidal streams.*

Accepted Manuscript
Version of record at: https://doi.org/10.1111/gwat.13274

Abstract

Coastal agricultural zones are experiencing salinization due to accelerating rates of sea-level rise (SLR), causing reduction in crop yields and abandonment of farmland. Understanding mechanisms and drivers of this seawater intrusion (SWI) is key to mitigating its effects and predicting future vulnerability of groundwater resources to salinization. We implemented a monitoring network of pressure and specific conductivity (SC) sensors in wells and surface waters to target marsh-adjacent agricultural areas in greater Dover, Delaware. Recorded water levels and SC over a period of three years show that the mechanisms and timescales of SWI are controlled by local hydrology, geomorphology, and geology. Monitored wells did not indicate widespread salinization of deep groundwater in the surficial aquifer. However, monitored surface water bodies and shallow (<4 m deep) wells did show SC fluctuations due to tides and storm events, in one case leading to salinization of deeper (18 m deep) groundwater. Seasonal peaks in SC occurred during late summer months. Seasonal and interannual variation of SC was also influenced by relative sea level. The data collected in this study data highlight the mechanisms by which surface water-groundwater connections lead to salinization of aquifers inland, before SWI is detected in deeper groundwater nearer the coastline. Sharing of our data with stakeholders has led to the implementation of SWI mitigation efforts, illustrating the importance of strategic monitoring and stakeholder engagement to support coastal resilience.

Accepted Manuscript
Version of record at: https://doi.org/10.1111/gwat.13274

Introduction

Approximately 40% of the global population (United Nations 2017) and 20% of all cropland (Teluguntla et al. 2016) lie within 100 km of one of the largest potential sources of contamination to freshwater – saltwater. Coastal zones are vulnerable to seawater intrusion (SWI) due to sea-level rise (SLR), more intense and frequent storm surges, and human activities, such as pumping and land use change, which result in salinization of soils, surface water, and groundwater (White and Kaplan 2017; Tully et al. 2019a). In low-lying areas such as the Mekong Delta in Vietnam and New Orleans, LA, USA, SWI has already contributed to hundreds of millions of dollars (USD) in economic losses (Williams 2010; Global Facility for Disaster Reduction and Recovery 2017). Understanding the mechanisms and drivers of salinization is key to effective mitigation and prediction of future vulnerability.

Coastal communities have been dealing with SWI into their aquifers for over a century (Barlow and Reichard 2010), and studies have reported SWI on every inhabited continent (e.g., Van Camp et al. 2014; Datta, Vennalakanti, and Dhar 2009; Costall et al. 2020; Lovrinovi et al. 2021; Barlow and Reichard 2010; Carretero et al. 2013). The two most studied mechanisms of SWI are 1- subsurface, lateral intrusion of seawater into freshwater aquifers driven by rising sea levels (e.g., Werner and Simmons 2009; Chang et al. 2011; Carretero et al. 2013), and groundwater pumping (e.g., Cummings 1971; Yu and Michael 2019); and 2- surface inundation from storm surges (e.g., Tebaldi, Strauss, and Zervas 2012; Yu et al. 2016). Subsurface SWI due to long-timescale SLR and pumping has been widely monitored (e.g., Demirel 2004; Prinos et al. 2014). Observations of episodic salinization of groundwater from storm surges are rarer. Several studies have focused on the aftermath of surges from large, catastrophic storms like Hurricanes Katrina

Accepted Manuscript
Version of record at: https://doi.org/10.1111/gwat.13274

and Rita (e.g., Farris et al. 2007; Williams 2010) and the 2004 tsunami in the Indian ocean (Illangasekare et al. 2006; Vithanage et al. 2012; Chinnasamy and Sunde 2016). As such events were not necessarily predicted, field measurements of salinity were gathered from existing monitoring well networks that were not strategically designed to capture the long-term, driving mechanisms of SWI, but rather only highlight the extent of salinization of singular events.

In the past several years, there has been growth in the scientific literature that focuses on increased frequency of nuisance flooding (i.e. minor tidal floods) due to SLR (Moftakhari et al. 2015; Karegar et al. 2017; Jacobs et al. 2018). However, most of these studies focus only on the impact and extent of the submersion of the land, not residual effects from the salinization of surface and groundwater. Studies that have examined the impacts of repeated salinization events have primarily been conducted from an ecological perspective and have been limited to shallow groundwater (e.g., Herbert et al. 2015; Tully et al. 2019b; Gedan and Fernández-Pascual 2019), leaving the physical hydrological mechanisms by which the SWI occurs poorly characterized.

Most rivers and streams are hydraulically connected to aquifers (Winter et al. 1998), and along the coast, the competing forces of tides and freshwater inputs shift the position of the freshwater-saltwater interface in streams (Gong and Shen, 2011). Both rising sea levels (Manda et al. 2014; Smajgl et al. 2015) and streamflow reduction due to reduced precipitation and groundwater pumping cause upstream migration of the salt front in streams (DRBC 2019; Wolock et al. 1993; Peters et al. 2022) . The salinized surface water could pose a threat to fresh groundwater beneath streams that are losing water to the aquifer, either naturally or due to nearby pumping (Navoy et al. 2005), or if saline water becomes trapped behind an impoundment and migrates into the subsurface (e.g., Nuruzzaman et al. 2014). There is a need for studies that

examine long-term drivers of SWI, episodic flooding events, and surface water-groundwater connections to understand how these processes and linkages may initiate and compound salinization of groundwater.

The aim of this study was to gain increased understanding of the mechanisms and timescales of salinization and freshening of surface water and groundwater in a coastal, agricultural region. For the purposes of this study, we define currently salinized locations as those with sustained specific conductivity (SC) levels above 1 mS/cm, and salinization events to be where the with SC increases by at least 1 mS/cm within the respected timescale of the driver (i.e. within hours for tidal fluctuations and months for seasonal variations). We selected 1 mS/cm as that is the equivalent to 2% seawater and 250 ppm chloride, which is the EPA's secondary maximum contaminant level for drinking water. Multiple tidal channels, marshes, irrigation ponds, and monitoring wells along the border between agricultural fields and tidal channels and marshes were equipped with data loggers to record the fluctuations and trends in water levels and specific conductivity between April 2018 and October 2021. Collected data were compared with precipitation, tidal, and sea-level data to link the observed changes with drivers of SWI. Increased understanding of how mechanisms and primary drivers of SWI vary spatially and temporally will aid in developing targeted SWI-monitoring programs, designing mitigation strategies, and predicting future SWI in other vulnerable coastal zones.

Study Area

The study area centers around the agricultural land east of the city of Dover, Delaware, with field monitoring sites lying between Dover and Delaware Bay (Figure 1). The farmland in this area is fringed by saline to brackish marshland to the east and dissected by tidal stream channels.

In this work, we refer to flowing water that exhibited a semi-diurnal tidal fluctuation in water levels and SC as tidal channels and rivers, and to standing water that varies tidally as marshes. Several man-made irrigation ponds are located adjacent to the marsh areas. These ponds partially penetrate the surficial Columbia aquifer (Columbia) and intersect the water table, making them surface expressions of groundwater. The Columbia is composed mainly of fine to coarse sand with discontinuous lenses of gravel and mud beds which range in age from Pliocene to Holocene (Mclaughlin and Velez 2006). While the Columbia is generally described as an unconfined aquifer, extensive subsurface data have identified mud beds in some areas, which may cause localized confined conditions (Andres 2004; Mclaughlin and Velez 2006; Andres et al. 2019). These muddy beds potentially separate the Columbia into shallower and deeper portions, which could give rise to the formation of two different freshwater-saltwater interfaces in some areas. Approximately 90% of all irrigation water in the study area is sourced from the Columbia. Dover obtains approximately 12% of its public water supply from the Columbia, relying on the deeper, confined Cheswold and Piney Point aquifers for the majority of its water (WRA 2021). Growing competition for groundwater combined with proximity to the coast, low elevation, and a faster than average local rate of SLR (Engelhart, Peltier, and Horton 2011) puts greater Dover's freshwater resources at high risk of contamination from SWI. A groundwater modeling study by He and Andres (2018) found that increasing the withdrawals from public and irrigation wells completed in the surficial aquifer would reverse groundwater flow and induce losing conditions from marshes and streams. The results of that study were used to determine which locations were at highest risk of salinization – groundwater adjacent to a saltwater body that may experience drawdown to 0.5 m above sea level or less; these areas were targeted for instrumentation in this work.

Accepted Manuscript
Version of record at: https://doi.org/10.1111/gwat.13274

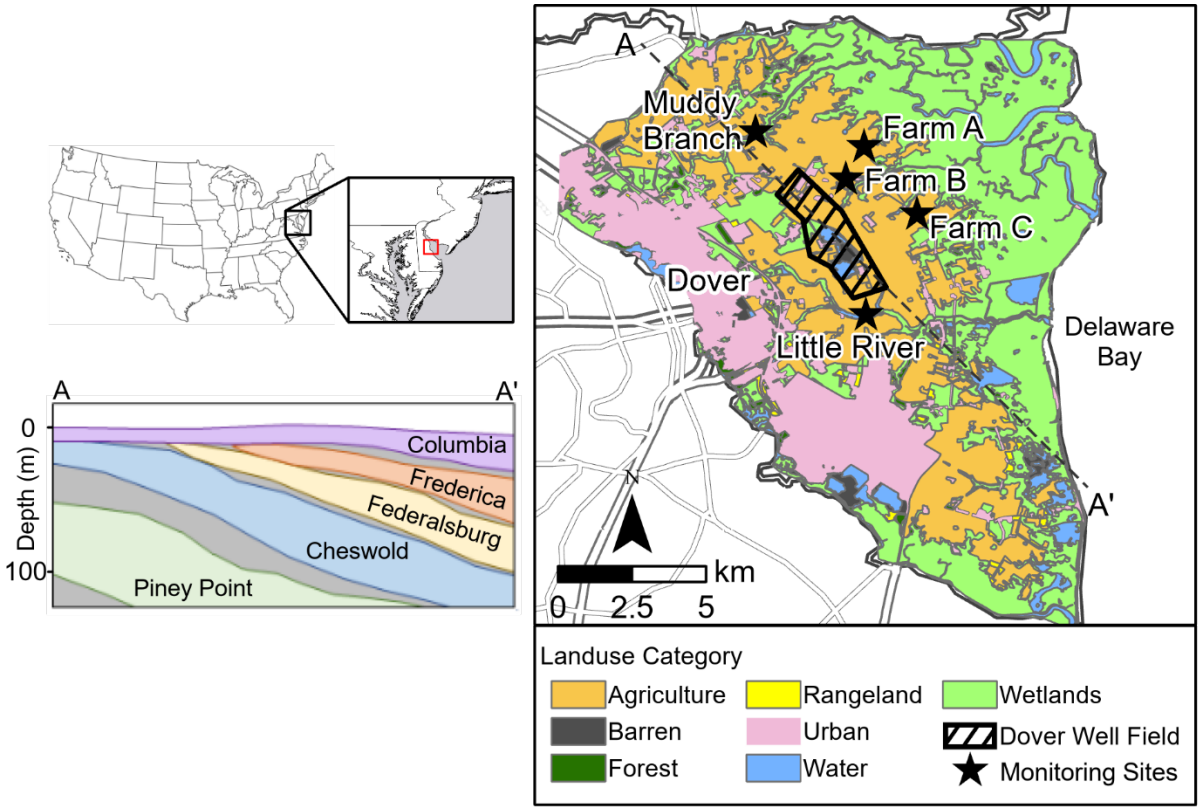

Figure 1. (A) Map of study area, highlighting the land use, monitoring sites (stars) and location of Dover's Columbia Aquifer water supply wells. (**B)** Simplified cross-section of the hydrostratigraphy underlying the study area.

Methods

Solinst LTC Leveloggers and In-Situ AquaTROLLs (both referred to as loggers) were deployed in existing test wells, newly constructed monitoring wells, and surface water bodies in the east Dover region to monitor hydraulic pressure, conductivity and temperature. While the AquaTROLLs automatically correct for differences in water level due to density, the Solinst Leveloggers do not; a manual correction was applied to Solinst data after downloading to report water levels as equivalent freshwater heads. In the shallow wells, loggers were hung

approximately 0.3 m above the bottom of the screen. In deep wells, either two loggers were initially installed at the top and bottom of the screen, or a logger recording SC at 10 second intervals was lowered down the well to assess for stratification. As the deep and shallow loggers did not show a significant difference, we have only reported the deep logger values for simplification. The temperature-correction equation found in the In-Situ Inc. manual was applied to the conductivity measurements and data are reported here as specific conductance (SC) (APHA 2005). Table 1 provides details on the monitoring locations and well construction information. Automated groundwater level data were collected at 15-minute intervals and managed using procedures documented by Andres et al. (2019). Logger data were downloaded approximately every three to four months. During each field visit, manual depth-to-water measurements were collected using an electronic water level meter in wells and from staff gages in surface waters and used to remove drift or offset from the recorded logger pressure data. Loggers used during this project were non-vented and all pressure measurements were adjusted for atmospheric pressure fluctuations using barometric pressure collected from a local climate station (DEOS 2021). All conductivity loggers were initially calibrated to standard specific conductivity solutions appropriate for the expected maximum salinities at each site and then recalibrated based on observed salinities. Ground surface and measuring point elevations were surveyed using real-time kinematic (RTK) positioning equipment in order to convert pressure measurements and depth to water levels to elevations (meters NAVD88). To prevent damage from freezing, loggers were removed from the marshes during winter months (December – March), resulting in data gaps.

Site Descriptions

Farm A

Accepted Manuscript
Version of record at: https://doi.org/10.1111/gwat.13274

Farm A irrigates crops with water from an irrigation pond that is adjacent to a tidal marsh (Figure 2). The depth of the pond is estimated to be 3 to 5 m, and partially penetrates the Columbia aquifer. Loggers were deployed in Pond A and Marsh A between April 2018 and October 2021. When the loggers were first deployed, there was no constructed barrier between the edge of the marsh and pond. The two locations were separated by approximately 10 m with no significant difference in ground surface elevation (Table 1, Figure 2). Construction of an earth fill dam and flashboard-riser water control structure in April 2020 caused the marsh area to fill in with sand, burying the logger. As this changed the hydrologic setting from the initial set-up, data from Marsh A after April 2020 are not reported.

Farm B

Situated just south of Farm A, Farm B also uses a dug pond as its irrigation water source (Figure 2). The pond (Pond B) is separated from a tidal marsh (Marsh B) by a 3-m wide berm; however, a 0.61-m diameter pipe runs through the berm, allowing water to freely flow between the pond and marsh. Pond B and Marsh B were equipped with loggers in April 2018. Two monitoring wells screening different depth intervals (4.5-7.6 m and 15.2-18.3 m) were installed through the berm in the summer of 2018 and equipped with loggers.

Farm C

For irrigation, Farm C irrigated with water pumped from three wells around the property that are piped into a single center pivot sprinkler system (Figure 2). Test wells were installed within 3 m of the irrigation well sites prior to construction of the irrigation wells and this study. Corresponding irrigation wells and test wells have similar the same screened intervals (Table 1). Test wells (DW-C1, DW-C2, and DW-C3) were equipped with loggers in June 2019. Monitoring well

Accepted Manuscript
Version of record at: https://doi.org/10.1111/gwat.13274

(DW-C4), of similar design to the test and irrigation wells was installed along the northern edge of the cultivated land during this study. Three shallow monitoring wells were installed along the northern and eastern edges of the property; SW-C2 and SW-C3 were drilled to approximately 3.6 m deep, and SW-C1 was hand-augured to 3.1 m deep (Figure 2). A tidal monitoring station (TC-C) consisting of a logger attached to a rod was installed in the tidal channel that borders the northern edge of the property. Due to difficulty accessing TC-C, the logger only operated from August 2019 to August 2020.

Muddy Branch

A logger was installed in Muddy Branch a tidal creek located approximately 15 km upstream from the river's mouth on the Delaware Bay (Figure 2). The logger was located in a perforated PVC pipe that was attached to the wing wall of a bridge.

Little River

An earth-fill dam with concrete weir exists along the Little River to create an irrigation source and limit tidal influence (Figure 2). The weir is approximately 1 m high. Though used as an irrigation pond, because the river extends over 3 km further inland, data from Little River are grouped with the other tidal channels. A logger was deployed approximately 400 m upstream from the dam in August 2019, next to the pond irrigation pump.

Accepted Manuscript
Version of record at: https://doi.org/10.1111/gwat.13274

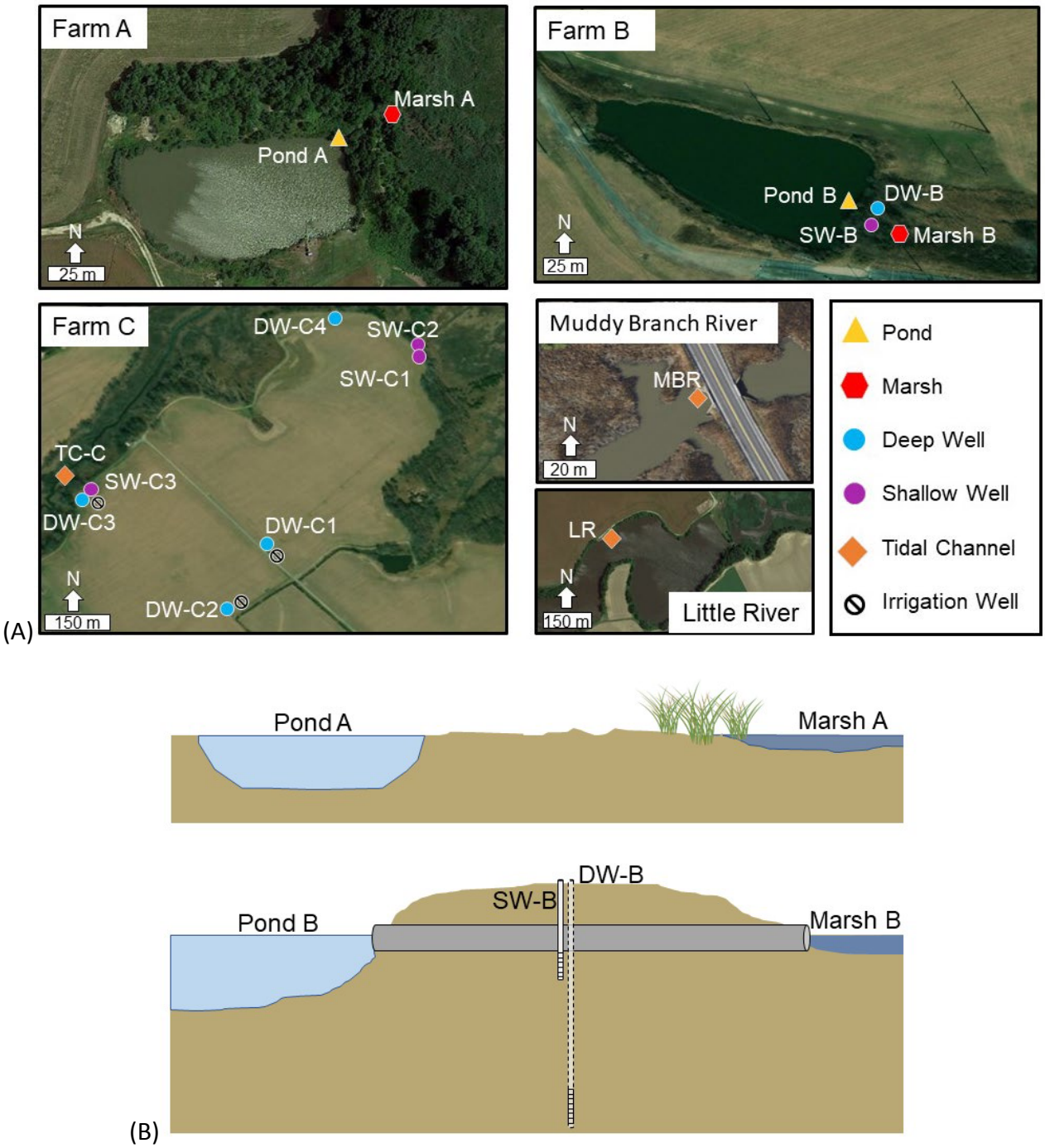

Figure 2. (A) Site layouts of monitoring points. **(B)** Simplified schematics of Farm A (top) and Farm B (bottom), not to scale.

Accepted Manuscript
Version of record at: https://doi.org/10.1111/gwat.13274

Table 1. Monitoring set-up descriptions and well construction information (bgs: below ground surface) *Ground surface elevation adjacent to surface water body. ^ Indicates wells equipped with In-Situ Aqua Trolls; all other wells were equipped with Solinst Leveloggers.

Site	Monitoring ID	Description	Ground Surface Elevation (m NAVD88)	Total Depth (m bgs)	Screened Interval (m bgs)	Linear Map Distance to Coast (km)	Date Logger Deployed
Farm A	Pond A	Irrigation Pond	0.64*	--	--	5.6	Apr. 2018
	Marsh A	Marsh	0.65	--	--	5.6	Apr. 2018
Farm B	Pond B	Irrigation Pond	0.81*	--	--	6.2	Apr. 2018
	Marsh B	Marsh	1.16	--	--	6.2	Apr. 2018
	DW-B	Monitoring Well	2.59	18.3	15.2 - 18.3	6.2	June 2018^
	SW-B	Monitoring Well	2.59	7.6	4.5 - 7.6	6.2	June 2018^
Farm C	DW-C1	Existing Test Well	4.07	24.4	6.1 - 21.3	4.4	June 2019
	DW-C2	Existing Test Well	3.53	30.5	6.1 - 22.9	4.5	June 2019
	DW-C3	Existing Test Well	2.29	27.4	11.9 - 24.1	4.8	June 2019
	DW-C4	Monitoring Well	1.21	19.0	9.5 - 18.6	4.2	June 2019
	SW-C1	Monitoring Well	1.73	3.6	2.1 - 3.7	4.0	Aug. 2019
	SW-C2	Monitoring Well	1.22	3.1	1.4 - 2.9	4.0	Aug. 2019
	SW-C3	Monitoring Well	2.17	3.6	2.1 - 3.7	4.8	Aug. 2019
	TC-C	Tidal Channel	-0.28	--	--	4.8	Aug. 2019
Muddy Branch	MBR	Tidal Channel	1.34*	--	--	9.1	July 2019
Little River	LR	Irrigation Pond	0.31*	--	--	4.9	June 2019

Accepted Manuscript
Version of record at: https://doi.org/10.1111/gwat.13274

Results

Plots of 15-minute interval data provided online in Supporting Information (Figures S1 – S5).

Tidal Channels

Water levels and SC in the Muddy Branch and TC-C showed strong semidiurnal tidal signals. Little River water levels also fluctuated diurnally, but SC showed only a high-spring tide signal (Figure 3, Figure S1). Seasonal trends of high SC in late summer/early fall and low SC in late winter were observed at these three locations. Average SC values from March through May were 4.8 mS/cm, 7.4 mS/cm, and 0.85 mS/cm for Muddy Branch, TC-C and Little River, respectively. From August through October, averages increased to 11.7 mS/cm in Muddy Branch, 15.3 mS/cm in TC-C, and 2.8 mS/cm in Little River. Water levels in Little River were responsive to precipitation events, but the tidal signals in Muddy Branch and the Farm C tidal channel overwhelmed any increases due to precipitation (Figure 3). Average SC was highest at all three locations during the summer and fall of 2019 when precipitation was lower than normal and sea level was higher than average (Figure 3). Maximum SC levels at all three sites aligned with the storm surge caused by Tropical Storm Melissa (Melissa) in October 2019. Coinciding with a high spring tide, Melissa caused inundation up to 1 m above ground surface along the Delaware coast which mainly flooded the marshland but did not flood our monitored farmland areas; however we cannot comment on if it flooded other farms in the study area (Berg 2019).

Farm A

Prior to the spring of 2020, both Marsh A and Pond A exhibited tidal, seasonal and interannual increases in SC (Figure 3; Figure S2). Large drops in water level in Pond A were due to

Accepted Manuscript
Version of record at: https://doi.org/10.1111/gwat.13274

pumping from the pond between June and October of each year (Figure 3). Rapid increases in SC in Marsh A and Pond A occurred during spring high tides. While 2018 (1558 mm rainfall) and 2020 (1426 mm rainfall) were relatively wet years, 2019 (1134 mm rainfall) and 2021 (1145 mm rainfall) were drier, with below-average (1216 mm) total precipitation (Figure 3) (NERRS Data). Below normal rainfall in summer 2019 led to a total farmer-reported pumping of 36,823 cubic meters from Pond A, compared to 21,140 cubic meters in 2020 (water usage was not reported in 2018 from Pond A and 2021 volumes have not been reported at the time of publication; data provided by Delaware Dept. of Natural Resources and Environmental Control). In August 2019, there was no overland flow from the marsh into the pond, there was a coincident increase in SC from about 3.1 mS/cm to 8.6 mS/cm in Pond A that continued as the water level recovered from pumping. The magnitude of increase in SC and the simultaneous increase in water level suggests the increase in SC was not due to evaporation but to saline groundwater flowing into the pond (Figure 4). An increase in SC also occurred when Melissa passed off the coast on October 11, 2019, which caused a significant storm surge and coastal flooding (Figure 3).

After sharing collected data with Farmer A, an earth-fill dam and water control structure was installed in the spring of 2020. Following the installation, water levels in Pond A rose approximately 0.5 m and there was no seasonal increase in SC in Pond A during the 2020 or 2021 irrigation seasons (Figure 3). Similarly, rapid increases of SC in Marsh A occurring in 2020 and 2021 had no associated increases of SC in Pond A.

Farm B

Farm B had not experienced any sustained (i.e. longer than a day) increases in SC until Melissa. Prior to Melissa, large fluctuations in SC were limited to 5 acute, episodic events in Pond B

Accepted Manuscript
Version of record at: https://doi.org/10.1111/gwat.13274

and Marsh B which corresponded to high spring tides (Figure 3; Figure S3). During these short-lived events, SC in the marsh increased to up to 10 mS/cm, but returned to base levels around 0.2 mS/cm within about 3 hours. Diurnal tidal fluctuations were seen in water levels in the wells (+/- 0.05 m in DW-B and +/- 0.015 m in SW-B), but were only sporadically recorded (+/- 0.005 m) in Marsh B and Pond B, indicating an intermittent connection between Marsh B and Pond B with the nearby tidal channel. Rapid decreases in water levels due to pumping of Pond B can be seen in adjacent Marsh B, DW-B, and SW-B indicating connectivity between surface water and groundwater (Figure 3).

SC in Marsh B spiked to almost 28 mS/cm during Melissa (Figure 5). Marsh B water levels were high enough to allow the brackish water to flow through the pipe into Pond B and increase SC to almost 4.2 mS/cm. Marsh B SC recovered relatively quickly after the initial surge; however, a slower, secondary increase in SC occurred as the salty water began draining out of Pond B. SC in Pond B remained elevated for an extended period of time, and after 6 months had only decreased to about 2.1 mS/cm. Approximately 3 days after the increase in SC in Pond B, SC in SW-B, screened 4.5 m below land surface, began to increase. SC in SW-B reached a peak of about 2.1 mS/cm on November 2nd, after which SC in both Pond B and SW-B began to slowly decrease. In mid-January 2020, SC in DW-B, screened 10.7 m below SW-B, began to increase. Before Melissa, SC was below 0.3 mS/cm in all four monitoring points, but still in May 2020, seven months after the surge, SC in SW-B remained approximately 1.2 mS/cm, while Pond B had an SC of 0.6 mS/cm and DW-B was at 0.3 mS/cm (Figure 5).

Farm C

Shallow Wells

Accepted Manuscript
Version of record at: https://doi.org/10.1111/gwat.13274

Water levels in the three shallow wells (SW-C1, SW-C2, and SW-C3) on Farm C were very similar. SC in SW-C1 and SW-C3 were below 0.5 mS/cm with no discernable trends, but, SW-C2, located on the edge of the marsh, had an average SC of 4.2 mS/cm and experienced large seasonal increases in SC (Figure 3; Figure S4). SW-C2 had peak SC over 20 mS/cm during the fall of 2019, coinciding with Melissa (Figure 3). No increase in SC was observed in SW-C1 despite being located only 20 m inland from SW-C2, likely due to its 0.5-m higher elevation.

Deep Wells

DW-C1, DW-C2 and DW-C3, which are adjacent to the irrigation wells, showed short-term pumping responses in both water level and SC, but no long-term significant changes were found (Figure 3; Figure S5). SC decreased simultaneously with the onset of pumping and increased with the cessation of pumping. Since all the SC levels in these deep wells were below 0.4 mS/cm, and recovered to non-pumping levels immediately following the cessation of pumping, these short-term fluctuations are assumed to be due to disturbance of non-seawater solutes sourced from the surface (i.e. fertilizer) and localized stratification of those solutes. A more detailed explanation of the effects of pumping dynamics on individual well SC levels can be found in McQuiggan et al. (*In press*). Limited drawdown in water levels (i.e <0.7 m drawdown) was observed in DW-C4 when the average non-pumping water levels of the other deep wells were below 1.5 m NAVD 88 and two or more wells were pumping for at least 24 hours. These conditions occurred most frequently in 2019 when average water levels were at their lowest during the study period and not during 2020 when water levels were at their highest. During summer irrigation of 2020 and 2021, there was a slight (~0.06 mS/cm) seasonal increase in DW-C4 SC levels. Given the proximity to the marsh but small magnitude of this change and a lack of data from the first half of the 2019 irrigation period, we

cannot discern if this seasonal increase is due to vertical migration of solutes from the surface or lateral migration of brackish water from beneath the marsh. The wells DW-C3 and DW-C4, located closest to the tidal channel showed clear tidal signals in their water levels but not in SC (Figure 3).

Accepted Manuscript
Version of record at: https://doi.org/10.1111/gwat.13274

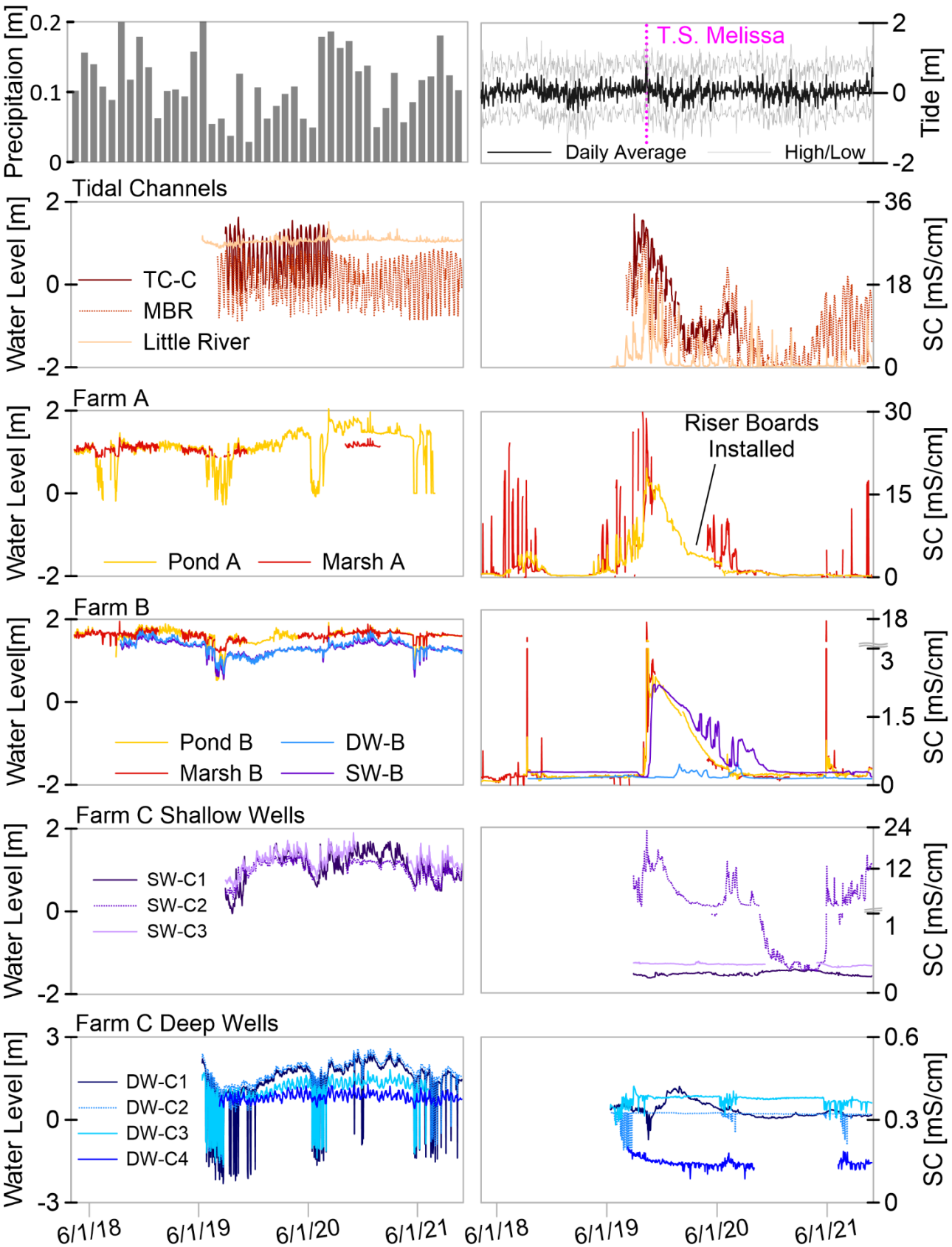

Accepted Manuscript
Version of record at: https://doi.org/10.1111/gwat.13274

Figure 3. Top panels show total monthly precipitation (left) and daily tide levels (right). Daily average water levels relative to NAVD88 are shown in the left-side panels and daily average specific conductivity (SC) are shown in the right-side panels for all monitoring locations. Note y-axis rescaled at 3 mS/cm for Farm B SC and at 1 mS/cm for Farm C shallow wells. Precipitation data were obtained from NOAA National Estuarine Research Reserve System for the St. Jones station, and tidal data was from the NOAA tide gauge 8537121 Ship John Shoal, NJ.

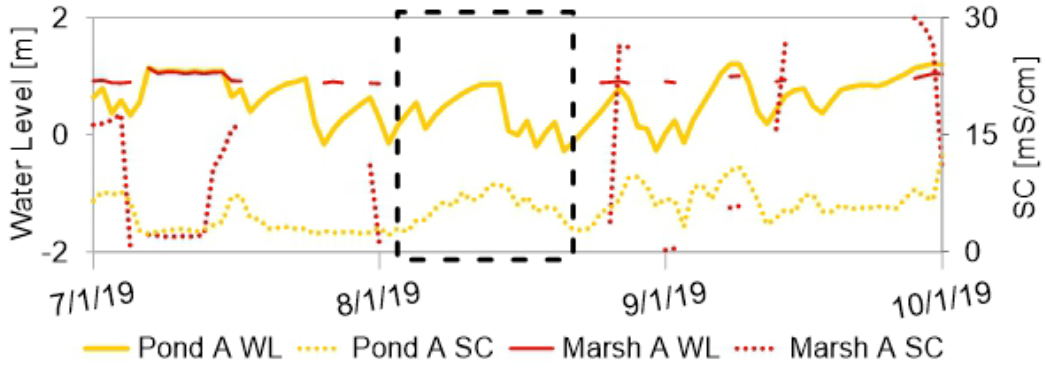

Figure 4. Water levels and SC from Farm A during the period in 2019 when Marsh A became dry while SC levels in Pond A increased, indicating flow of brackish groundwater into the pond.

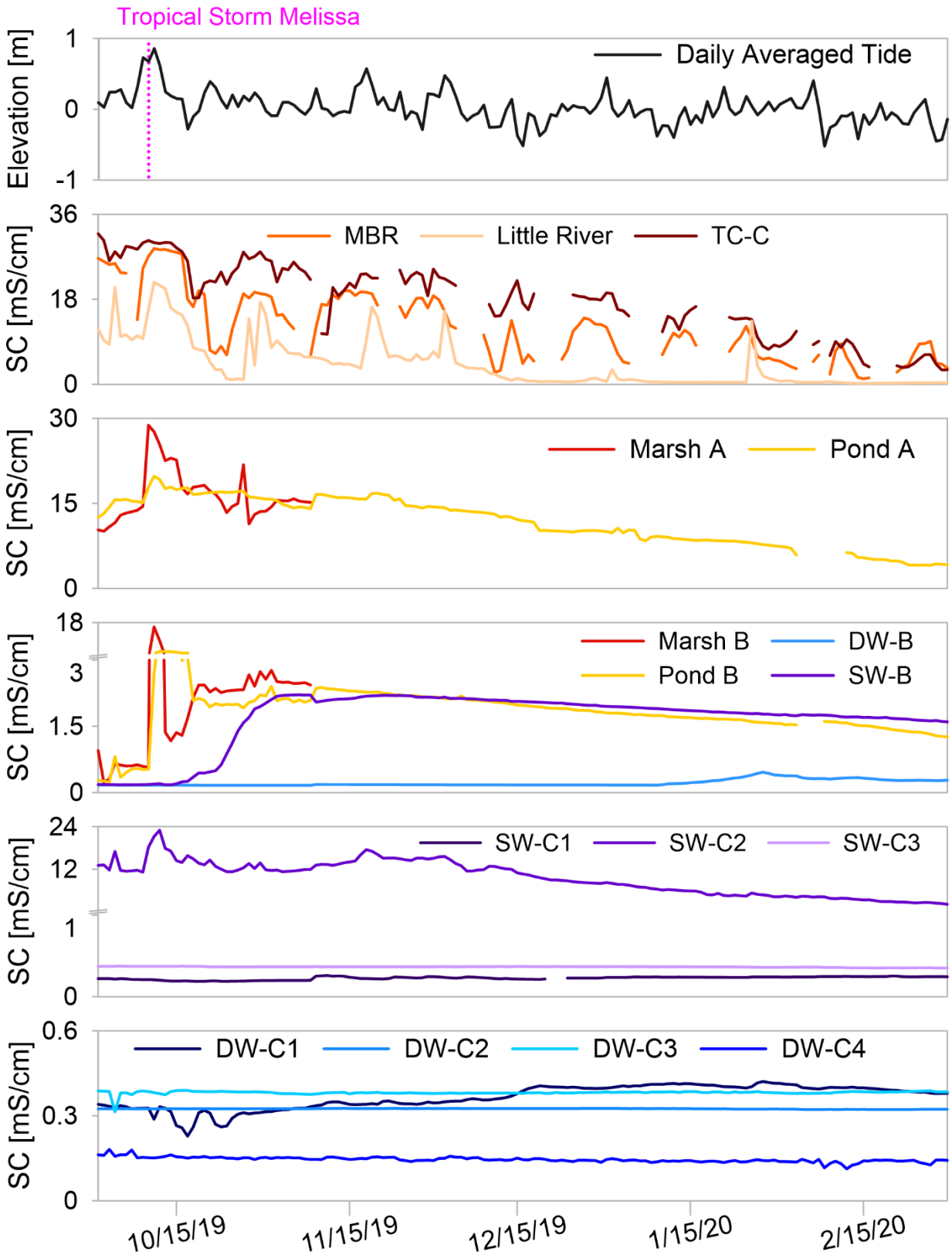

Accepted Manuscript
Version of record at: https://doi.org/10.1111/gwat.13274

Figure 5. Daily tide levels, referenced to NAVD88, and specific conductivity (SC) from all monitoring sites starting from 10 days before to 5 months after the passing of Tropical Storm Melissa. Immediate increases in SC can be seen in all surface water bodies and SW-C2. Note re-scale of y-axes on the Farm B plot at 3 mS/cm and the Farm C shallow wells plot at 1 mS/cm.

Discussion

Primary pathways, mechanisms, and timescales of SWI vary by location and depend on distance from and connectivity to surface water, topography, and site-specific geology. Though widespread deep SWI was not observed, data showed temporally and spatially diverse patterns of salinization at each site and suggest the likely occurrence of two, shallow and deep, saltwater-freshwater transition zones within the Columbia Aquifer.

Pathways and Mechanisms of Salinization

Surface water-groundwater connections can serve as pathways for inland salinization of deep groundwater. Figure 6 represents a simplified layout of the Dover region and the observed and potential pathways and mechanisms of SWI. The top panel of Figure 6 shows how the irrigated farmland is located between the channelized marshland and Dover, with a larger tidal stream extending farther inland.

The semi-circle crop in panels Ia and IIa of Figure 6 is irrigated by a well located near the edge of the marsh. The cross-sectional IIa panel shows how saline water that floods the marsh area could infiltrate into the deeper groundwater if it reaches the edge of a discontinuous shallow confining unit or low-permeability sediments that typically underlie marshes (Xin et al. 2012;

Accepted Manuscript
Version of record at: https://doi.org/10.1111/gwat.13274

Guimond and Tamborski 2021). A shallow (<4 m bgs) clay layer was observed during installation of the three shallow monitoring wells and DW-C4 at Farm C, and the drilling log for DW-C3 also reported a clay layer at 5 m bgs. No clay layer of a similar depth was reported in the two more inland, deep wells, DW-C1 and DW-C2. This indicates the clay layer terminates somewhere beneath the cropped area. Shallow, low-permeability units may currently protect deeper groundwater from saltwater infiltration due to surface inundation; however, SLR and high storm surges may push saltwater beyond the extent of these limited confining units, leading to SWI of deep groundwater. Additionally, a shallow confining unit could lead to two separate freshwater-saltwater interface zones. While the deeper interface may be slower to advance inland, repeated inundation of the ground surface by saltwater from storm surges could lead to rapid and chronic salinization of the shallow zone leading to die-off of crops and vegetation (e.g., Kirwan and Gedan, 2019.; Tully et al. 2019a). Evidence of such salinized shallow groundwater was recorded at Farm C in SW-C2 (Figures 3 and 4). At SW-C2, elevated SC was driven by seasonal increases in sea level and storm surge from Melissa. When installing new wells, especially those of high pumping capacity, they should be located as far away from the edge of marshes as possible to reduce vulnerability from pumping-induced flow of salinized, shallow groundwater.

In panels IIa and IIb of Figure 6, moving inland from the marsh, there is a small irrigation well near the coastline, a larger irrigation well further inland, and large municipal wells farthest inland, all bordered by a river to the north. Barlow and Leake (2012) highlighted how groundwater pumping can pull stream water into the underlying aquifer, and Peters et al. (2022) used an analytical model to show how increased groundwater pumping can cause salt fronts to migrate farther inland in coastal rivers. Thus, it is reasonable to conclude that SWI may be induced due to

Accepted Manuscript
Version of record at: https://doi.org/10.1111/gwat.13274

groundwater pumping near tidally-influenced streams. As shown in the SC data of the Muddy Branch, TC-C channel and Little River (Figure 3b), these coastal streams have a strong tidal signal and seasonal trends driven by sea level. While not observed in the collected data, the groundwater model of the east Dover area created by He and Andres (2018) showed that flow directions between surface water and groundwater could be locally altered, with previously gaining stream reaches becoming losing reaches, if 2015 permitted pumping rates by Dover were to doubled. If total withdrawals from the model were to occur, either solely by Dover or in combination with increased agricultural pumping, brackish surface water could be pulled into the groundwater. Additionally, increasing pumping rates at the municipal wells or larger irrigation wells could increase the risk of salinization of the smaller irrigation well that is located closer to the marsh from movement of the deeper saltwater-freshwater interface farther inland and pumping-induced upconing (Figure 6).

Panels Ic and IIc in Figure 6 represent agricultural operations, like Farms A and B, which rely on a groundwater-fed irrigation pond rather than standard wells. The schematics show how a direct connection between surface water and groundwater can salinize groundwater that is farther inland than the deeper, seaward freshwater-saltwater interface, and how the surface water could become salinized through subsurface SWI. Though irrigation ponds may not be as common as wells, coastal ponds and lakes geomorphologically similar to these are found throughout the world (Oertel 2005) and can retain saltwater following storm surge events, leading to infiltration of brackish water (Yu et al. 2016). Surface water acting as a conduit for salinization of groundwater was shown at Farm B, when a storm surge from Melissa coincided with high tide. This caused an increase in salinity in Marsh B, followed closely by connected Pond B. The high

surface water heads caused by the tide and surge likely reversed the hydraulic gradient, causing brackish pond water to flow into the aquifer, affecting the shallow groundwater within a few days. After three months, the brackish water eventually migrated deeper into the aquifer possibly due to density effects. In all, the observed salinization process occurred over several months, and recovery took approximately a year. As discussed in the Results and shown in Figure 4, Pond A experienced an increase in SC during a period when Marsh A was dry, indicating intrusion from brackish groundwater. Application of brackish water to the crops can, and did, result in reported reduced crop yield. Continued irrigation with brackish water can lead to salinization of the soil, reducing crop production in future growing seasons causing further ecological and economic impacts.

Timescales of Salinization

Large changes in SC were driven by sea-level fluctuations, which varied on multiple timescales (i.e. tides, storm surges, and seasonal changes in sea level mainly due to thermal expansion and contraction). Neither pumping nor precipitation had an obvious short-term impact on SC levels. Longer-term trends (i.e. monthly to seasonal) are more difficult to differentiate from the influence of sea level because precipitation dictates the amount of pumping, and both affect hydraulic heads. Periods of increased precipitation buffer the impact of higher sea levels, while drier periods compound the impacts. Monitoring sites that had strong tidally-influenced SC signals also displayed the greatest seasonal and interannual variation in SC caused, at least in part, by changes in monthly average sea level (Figure 3). A stronger and more frequent tidal signature indicates a more direct connection to the Delaware Bay. Anderson and Lockaby (2012) had previously observed that water levels and salinity in rivers and freshwater wetlands that

fluctuated with mean sea level showed greater tidally-induced fluctuations as well. Since SLR is one of the main consequences of climate change and increasing temperatures can increase the intensity of storm surges, areas that have stronger SC tidal signatures are, therefore, likely the locations which will experience climate-change-driven SWI first.

Generally, the decrease in SC following a salinization event, in both surface water and groundwater, occurred on the same timescale as the increase. For tides, SC increased within hours and then recovered within several hours to a day. Seasonal increases in sea level caused SC levels to gradually increase and decrease over a few months. The exception to this is the increase in SC due to storm surge. As previously discussed, the residual impacts of the Melissa surge were noticeable at Farm B for over a year after the storm (Figure 3) and caused SC to remain elevated above winter averages in the other surface water bodies and in SW-C2 (Figure 5). While storms can cause rapid salinization of inland surface water and groundwater, re-freshening of those sources takes much longer due to the magnitude of increase in salinity and decrease in the hydraulic gradient from flooding, resulting in a greater chance for compounding salinization from future SWI drivers.

Accepted Manuscript
Version of record at: https://doi.org/10.1111/gwat.13274

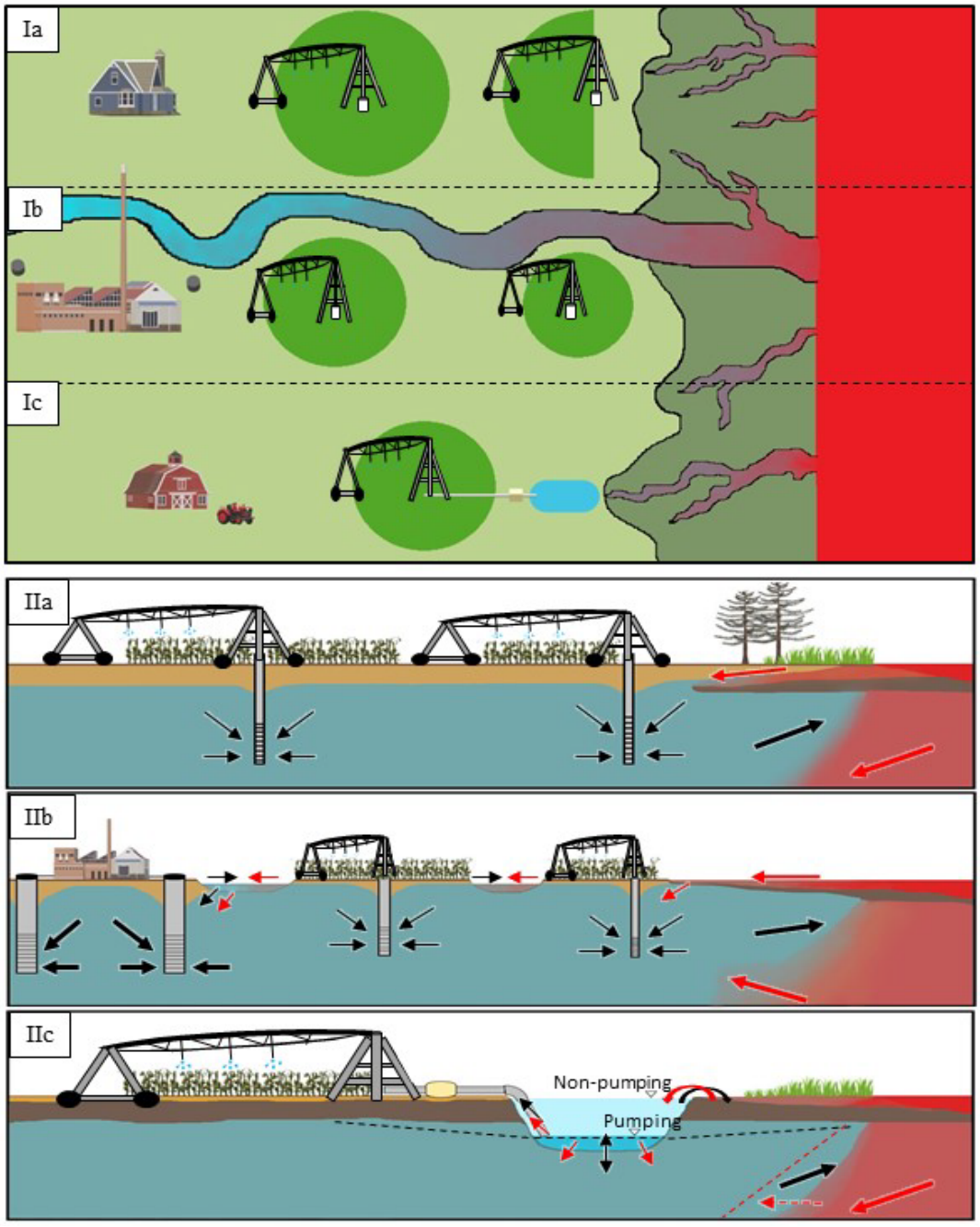

Figure 6. Schematic of water use distributions and salinization pathways. Panels (I) are simplified map views of the distribution of water users and water bodies in the Dover, Delaware area. The letters correspond to the cross-sectional panels (II) which illustrate mechanisms of SWI into the fresh groundwater. The relative size of the green crop irrigation circles corresponds to relative pumping amounts (i.e. wells in larger circles pump more water). Black arrows represent

Accepted Manuscript
Version of record at: https://doi.org/10.1111/gwat.13274

groundwater flow direction and red arrows signify the potential movement of saltwater due to a rise in sea level caused by high tides, storm surges and/or climate change, as well as reduction in freshwater hydraulic head from increased pumping. In panel IIc, the dashed lines represent water table elevation (black) and freshwater-saltwater interface (red) under pumping conditions.

Implications for Monitoring and Mitigation

The observed connections between surface water and groundwater have major implications for monitoring, modeling, and mitigation of SWI. We showed that sites near tidally-influenced surface water bodies, not just those closest to the coastline, are at risk of salinization. This should be taken into consideration when designing SWI monitoring networks in this region and in other coastal areas around the world. Additionally, surface water bodies need to be considered when creating numerical models for SWI. To reduce computational demand, two-dimensional models are often used to study SWI with the assumption that flow is only perpendicular to the coastline. When three-dimensional models are used, they also assume that sea boundary is the source of salinity and focus on monitoring the movement of the subsurface freshwater-saltwater interface. Failing to include salinized surface water bodies and pathways for surface intrusion of tides and storm surge via tidal channels in models may lead to an overestimation of the timing of occurrence of SWI and an underestimation of its spatial extent and magnitude.

Monitoring efforts coupled with communication of results are key to addressing current and future problems of SWI. Sharing our data with local stakeholders led to two major SWI mitigation efforts. First, by providing the landowners with regular updates about our findings, we were able to show Farmer A how and why the irrigation water was becoming salinized during

Accepted Manuscript
Version of record at: https://doi.org/10.1111/gwat.13274

irrigation season. They used this information to install a tidal gate to control the connection between Pond A and Marsh A. After installation, Pond A did not experience tidal or seasonal increases in SC, and the farmer did not report crop loss in 2020 or 2021. Secondly, we also shared our data at meetings with stakeholders, which included City engineers and officials, and land owners. After sharing that the most imminent risk of SWI would be to the surficial Columbia aquifer that is utilized by both the city of Dover and farmers, Dover altered its pumping regime by reducing withdrawals from the Columbia during irrigation season, to lessen competition with the farmers, and instead pumped more from the deeper, confined Cheswold aquifer (Figure 7). This has both improved coordination among groundwater users and increased the sustainability of its use.

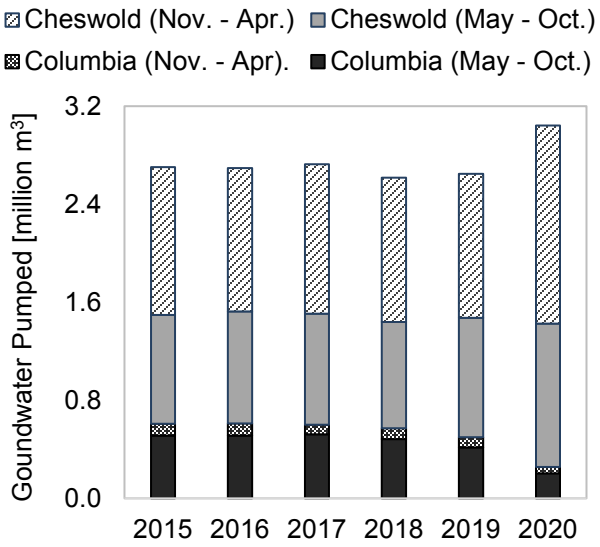

Figure 7. Groundwater withdrawals from the Columbia and Cheswold aquifers by the City of Dover during May – Oct., which coincides with irrigation by farmers, and Nov. – Dec. (*data provided by Delaware Dept. of Natural Resources and Environmental Control*).

Conclusion

This study assessed the current extent of salinization along a transition from marsh to agricultural land, along with the mechanisms and timescales of SWI. Water bodies and monitoring wells were equipped with pressure and specific conductivity loggers to determine the dominant timescales, pathways, and drivers of SWI. While we did not find widespread salinization of deeper groundwater, our data showed strong seasonal and interannual variations in salinity of shallow wells and surface waters driven by relative sea level and storm surge. This study also highlights that surface water bodies can act as pathways of SWI to deeper groundwater and in groundwater farther inland, away from the coastline, which should be considered in future SWI monitoring programs and groundwater modeling studies. Communication between researchers and stakeholders is also crucial to mitigate SWI. By regularly sharing our data with stakeholders and property owners, mitigation efforts have already been made to reduce the risk of salinization in the Dover, Delaware area. This work illustrates the importance of continuous and strategic monitoring and communication to improve understanding of drivers of SWI, develop effective mitigation measures, and improve resilience to coastal vulnerabilities.

Acknowledgements:

The authors would like to thank the landowners for allowing access to their properties and Steve McCreary for help with installation of the monitoring wells. All data cited in this paper can be found online as in CUAHSI Hydroshare [*citation will be provided on paper acceptance*]. This project was conducted as part of Project WiCCED (Water in the Changing Coastal Environment of Delaware), which is funded by the National Science Foundation EPSCoR Grant OIA1757353 and the State of Delaware. Funding for MH was also obtained from the Delaware Environmental Institute.

Supporting Information

Supporting information consisting of plots of 15-minute interval measurements of water levels and SC from the monitoring points can be found in the online version of this article. Supporting information is generally not subject to peer review.

References

Anderson, C. J., and B. G. Lockaby. 2012. Seasonal patterns of river connectivity and saltwater intrusion in tidal freshwater forested wetlands. *River Research and Applications*, *28* no. 7, 814-826. https://doi.org/10.1002/rra.

Andres, A. St. 2004. Groundwater recharge potential mapping in Kent and Sussex counties, Delaware. Delaware Geological Survey, Report of Investigations No. 66.

Andres, A. S., R. W. McQuiggan, C. He, and D. R. Wunsch. 2019. Kent County groundwater monitoring project: Results of subsurface exploration state of Delaware. Delaware Geological Survey, Open File Report No. 53.

APHA. 2005. Standard Methods for the Examination of Water and Wastewater, SM2520A, 21st ed. American Public Health Association/American Water Works Association/Water Environment Federation, Washington DC.

Barlow, P. M., and S. A. Leake. 2012. Streamflow depletion by wells-understanding and managing the effects of groundwater pumping on streamflow. U.S. Geological Survey Circular 1376. https://pubs.usgs.gov/circ/1376/.

Barlow, P. M., and E. G. Reichard. 2010. Saltwater intrusion in coastal regions of North America. *Hydrogeology Journal* 18 no. 1: 247–60. https://doi.org/10.1007/s10040-009-0514-3.

Berg, R. 2019. Tropical Storm Melissa. National Hurricane Center Tropical Cyclone Report AL 142019. https://www.nhc.noaa.gov/data/tcr/AL142019_Melissa.pdf.

Camp, M. V., Y. Mtoni, I. C. Mjemah, C. Bakundukize, and K. Walraevens. 2014. Investigating seawater intrusion due to groundwater pumping with schematic model simulations: the example of the Dar Es Salaam coastal aquifer in Tanzania. *Journal of African Earth Sciences* no. 96: 71–78. https://doi.org/10.1016/j.jafrearsci.2014.02.012.

Carretero, S., John R., H. Bokuniewicz, and E. Kruse. 2013. Impact of sea-level rise on saltwater intrusion length into the coastal aquifer, Partido de La Costa, Argentina. *Continental Shelf Research* 62–70. https://doi.org/10.1016/j.csr.2013.04.029.

Chang, S. W., T. P. Clement, M. J. Simpson, and K. K. Lee. 2011. Does sea-level rise have an impact on saltwater intrusion? *Advances in Water Resources* 34 no. 10: 1283–91. https://doi.org/10.1016/j.advwatres.2011.06.006.

Chinnasamy, P., and M. G. Sunde. 2016. Improving spatiotemporal groundwater estimates after natural disasters using remotely sensed data – a case study of the Indian Ocean Tsunami. *Earth Sciences Informatics no.* 9: 101–11. https://doi.org/10.1007/s12145-015-0238-y.

Costall, A. R., B. D. Harris, B. Teo, R. Schaa, F. M. Wagner, and J. P. Pigois. 2020. Groundwater throughflow and seawater intrusion in high quality coastal aquifers. *Scientific Reports* no. 10 (1): 1–33. https://doi.org/10.1038/s41598-020-66516-6.

Cummings, R G. 1971. Optimum Exploitation Groundwater Reserves with Saltwater Intrusion. *Water Resources Research* 7 no. 6, 1415-1424.

Datta, B., H. Vennalakanti, and A. Dhar. 2009. Modeling and control of saltwater intrusion in a coastal aquifer of Andhra Pradesh, India. *Journal of Hydro-Environment Research* no. 3: 148–59. https://doi.org/10.1016/j.jher.2009.09.002.

Demirel, Z. 2004. The history and evaluation of saltwater intrusion into a coastal aquifer in Mersin, Turkey. *Journal of Environmental Management* 70 no. 3: 275–82. https://doi.org/10.1016/J.JENVMAN.2003.12.007.

DEOS (Delaware Environmental Observing System). Accessed October 21, 2021. http://www.deos.udel.edu/data/daily_retrieval.php

Engelhart, S. E., W. R. Peltier, and B. P. Horton. 2011. Holocene relative sea-level changes and glacial isostatic adjustment of the U.S. Atlantic Coast. *Geology* 39 no. 8: 751–54. https://doi.org/10.1130/G31857.1.

Farris, G.S., G.J. Smith, M.P. Crane, C.R. Demas, L.L. Robbins, and D.L. Lavoie, eds. 2007. Science and the Storms: The USGS Response to the Hurricanes of 2005. U.S. Geological Survey Circular 1306. https://pubs.usgs.gov/circ/1306/.

Gedan, K. B., and E. Fernández-Pascual. 2019. Salt marsh migration into salinized agricultural fields: a novel assembly of plant communities. *Journal of Vegetation Science 30* no. 5, 1007-1016

Global Facility for Disaster Reduction and Recovery. 2017. Toward integrated disaster risk management in Vietnam recommendations based on the drought and saltwater intrusion crisis and the case for investing in longer-term resilience. Washington D.C. https://doi.org/10.1596/28871.

Gong, W., and J. Shen. 2011. The response of salt intrusion to changes in river discharge and tidal mixing during the dry season in the Modaomen Estuary, China. *Continental Shelf Research* 31 no. 7–8: 769–88. https://doi.org/10.1016/j.csr.2011.01.011.

Guimond, J, and J Tamborski. 2021. Salt marsh hydrogeology: A review. *Water 13* no. 4, 543. https://doi.org/10.3390/w13040543.

He, C., and A. S. Andres. 2018. Results of groundwater flow simulations in the east Dover Area, Delaware. Delaware Geological Survey, Open File Report. 52.

Herbert, E. R., P. B., A. J. Burgin, S. C. Neubauer, R. B. Franklin, M. A., K. N. Hopfensperger, L. P.M. Lamers, P. Gell, and J. A. Langley. 2015. A global perspective on wetland salinization: ecological consequences of a growing threat to freshwater wetlands. *Ecosphere* 6 no. 10, 1-43. https://doi.org/10.1890/ES14-00534.1.

Illangasekare, T., S. W. Tyler, T. P. Clement, K. G. Villholth, A. P.G.R.L. Perera, J. Obeysekera, A. Gunatilaka, et al. 2006. Impacts of the 2004 tsunami on groundwater resources in Sri Lanka. *Water Resources Research* 42 no. 5. https://doi.org/10.1029/2006WR004876.

Jacobs, J. M., L. R. Cattaneo, W. Sweet, and T. Mansfield. 2018. Recent and future outlooks for nuisance flooding impacts on roadways on the U.S. East Coast. *Transportation Research Record* 2672 no. 2: 1–10. https://doi.org/10.1177/0361198118756366.

Karegar, M. A, T. H. Dixon, R. Malservisi, J. Kusche, and S. E. Engelhart. 2017. Nuisance flooding and relative sea-level rise: the importance of present-day land motion. *Scientific Reports* 7 no. 1. https://doi.org/10.1038/s41598-017-11544-y.

Kirwan, M. L., and K. B. Gedan. 2019. Sea-level driven land conversion and the formation of ghost forests. *Nature Climate Change* 9 no. 6, 450-457. https://doi.org/10.1038/s41558-019-0488-7.

Lovrinovi, I., A. Bergamasco, V. Srzi, C. Cavallina, D. Holjevi, S. Donnici, J. Erceg, L. Zaggia, and L. Tosi. 2021. Groundwater monitoring systems to understand sea water intrusion dynamics in the Mediterranean: The Neretva Valley and the Southern Venice Coastal Aquifers case studies. *Water 13* no. 4, 561. https://doi.org/10.3390/w13040561.

Manda, A. K., A. S. Giuliano, and T. R. Allen. 2014. Influence of artificial channels on the source and extent of saline water intrusion in the wind tide dominated wetlands of the southern Albemarle estuarine system (USA). *Environmental Earth Sciences*, 71 no. 10, 4409-4419. https://doi.org/10.1007/s12665-013-2834-9.

Mclaughlin, P. P., and C. C. Velez. 2006. Geology and extent of the confined aquifers of Kent County, Delaware by geology and extent of the confined aquifers of Kent County, Delaware. Delaware Geological Survey, Report of Investigations No. 72.

McQuiggan, R., A. S. Andres, C. He, M. Hingst, T. McKenna, and H. A. Michael (in press). Kent County groundwater monitoring project: hydrogeology and salinization dynamics of eastern Kent County. Delaware Geological Survey, Report of Investigations No. 86.

Moftakhari, H. R., A. AghaKouchak, B. F. Sanders, D. L. Feldman, W. Sweet, R. A. Matthew, and A. Luke. 2015. Increased nuisance flooding along the coasts of the United States due to sea level rise: past and future. *Geophysical Research Letters* 42 no. 22: 9846–52. https://doi.org/10.1002/2015GL066072.

National Estuarine Research Reserve System (NERRS). 2003. System-Wide Monitoring Program. Data Accessed from the NOAA NERRS Centralized Data Management Office Website, 1–32. Accessed October, 10, 2021. https://doi.org/10.1201/9780203495605.ch1.

Navoy, A. S., L. M. Voronin, and E. Modica. 2005. *Vulnerability of production wells in the Potomac-Raritan-Magothy aquifer system to saltwater intrusion from the Delaware River in Camden, Gloucester, and Salem Counties, New Jersey*. U.S. Geological Survey Scientific Investigations Report 2011–5033. https://pubs.usgs.gov/sir/2011/5033/pdf/sir2011-5033.pdf

Nuruzzaman, A., F. Rabbi, M. Mahmuduzzaman, U. Ahmed, A. K. M. Nuruzzaman, and S. Ahmed. 2014. Causes of salinity intrusion in coastal belt of Bangladesh. *International Journal of Plant Research* no. 4A: 8–13. https://doi.org/10.5923/s.plant.201401.02.

Oertel, G. F. 2005. Coastal Lakes and Lagoons. *Encyclopedia of Earth Sciences* Series no. 14: 263–66. https://doi.org/10.1007/1-4020-3880-1_81.

Peters, C. N., C. Kimsal, R. S. Frederiks, A. Paldor, R. McQuiggan, and H. A. Michael. 2022. Groundwater pumping causes salinization of coastal streams due to baseflow depletion: analytical framework and application to Savannah River, GA. *Journal of Hydrology* no. 604: 127238. https://doi.org/10.1016/j.jhydrol.2021.127238.

Prinos, S. T., M. A. Wacker, K. J. Cunningham, and D. V. Fitterman. 2014. Origins and delineation of saltwater intrusion in the Biscayne Aquifer and changes in the distribution of saltwater in Miami-Dade County, Florida. U.S. Geological Survey Scientific Investigations Report 2014–5025. https://doi.org/10.3133/SIR20145025.

Smajgl, A., T. Q. Toan, D. K. Nhan, J. Ward, N. H. Trung, L. Q. Tri, V. P.D. Tri, and P. T. Vu. 2015. Responding to rising sea levels in the Mekong Delta. *Nature Climate Change* 5 no. 2: 167–74. https://doi.org/10.1038/nclimate2469.

DRBC. 2019. State of the Basin 2019. Delaware River Basin Commission. https://www.nj.gov/drbc/public/publications/SOTB2019.html

Tebaldi, C., B. H. Strauss, and C. E. Zervas. 2012. Modelling sea level rise impacts on storm surges along US coasts. *Environmental Research Letters* 7 no. 1. https://doi.org/10.1088/1748-9326/7/1/014032.

Teluguntla, P., P. Thenkabail, J. Xiong, M. Gumma, C. Giri, C. Milesi, M. Ozdogan, R. Congalton, J. Tilton, T. Sankey, R. Massey, A. Phalke, K. Yadav. Making Earth System Data Records for Use in Research Environments (MEaSUREs) Global Food Security Support Analysis Data (GFSAD) Crop Mask 2010 Global 1 km V001. 2016, distributed by NASA EOSDIS Land Processes DAAC, https://doi.org/10.5067/MEaSUREs/GFSAD/GFSAD1KCM.001. Accessed 2022-05-25.

Tully, K., K. Gedan, R. Epanchin-Niell, A. Strong, E. S. Bernhardt, T. Bendor, M. Mitchell, et al. 2019. The invisible flood: the chemistry, ecology, and social implications of coastal saltwater intrusion. *BioScience* 69 no. 5: 368–78. https://doi.org/10.1093/biosci/biz027.

United Nations. 2017. The Ocean Conference Factsheet: People and Oceans. New York.

Vithanage, M., P. Engesgaard, K. G. Villholth, and K. H. Jensen. 2012. The effects of the 2004 tsunami on a coastal aquifer in Sri Lanka. *Groundwater* 50 no. 5: 704–14. https://doi.org/10.1111/J.1745-6584.2011.00893.X.

Werner, A. D., and C. T. Simmons. 2009. Impact of sea-level rise on sea water intrusion in coastal aquifers. *Groundwater* 47 no. 2: 197–204. https://doi.org/10.1111/j.1745-6584.2008.00535.x.

White, E., and D. Kaplan. 2017. Restore or retreat? Saltwater intrusion and water management in coastal wetlands. *Ecosystem Health and Sustainability* 3 no. 1: 1–18. https://doi.org/10.1002/ehs2.1258.

Williams, V. J. 2010. Identifying the economic effects of salt water intrusion after Hurricane Katrina. *Journal of Sustainable Development 3* no.1, 29-37.

Winter, T., J. W. Harvey, O. L. Franke, W. M. Alley. 1998. *Ground water and surface water: a single resource*. U.S. Geological Survey Circular 1139.

Wolock, D. M., G. J. McCabe, G. D. Tasker, and M. E. Moss. 1993. Effects of climate change on water resources in the Delaware River Basin. *Journal of the American Water Resources Association* 29 no. 3: 475–86. https://doi.org/10.1111/j.1752-1688.1993.tb03225.x.

WRA (Whitman, Requardt & Associates LLP). 2021. Update to the Water Master Plan (Contract No. 21-0013WW) Final Report. City of Dover Delaware. https://www.cityofdover.com/departments/publicworks/UpdatetoWaterMasterPlanPresentation

Xin, P., J. Kong, L. Li, and D. A. Barry. 2012. Effects of soil stratigraphy on pore-water flow in a creek-marsh system. *Journal of Hydrology* no. 475: 175-187. https://doi.org/10.1016/j.jhydrol.2012.09.047.

Yu, X., and H. A. Michael. 2019. Mechanisms, configuration typology, and vulnerability of pumping-induced seawater intrusion in heterogeneous aquifers. *Advances in Water Resources* no. 128 (June): 117–28. https://doi.org/10.1016/j.advwatres.2019.04.013.

Yu, X., J. Yang, T. Graf, M. Koneshloo, M. A. O'Neal, and H. A. Michael. 2016. Impact of topography on groundwater salinization due to ocean surge inundation. *Water Resources Research* 52 no. 8: 5794–5812. https://doi.org/10.1002/2016WR018814.

List of Figures

Figure 1. Map of study area, highlighting the land use, monitoring sites (stars) and location of Dover's Columbia Aquifer water supply wells. B) Simplified cross-section of the hydrostratigraphy underlying the study area.

Accepted Manuscript
Version of record at: https://doi.org/10.1111/gwat.13274

Figure 2. (A) Site layouts of monitoring points. **(B)** Simplified schematics of Farm A (top) and Farm B (bottom), not to scale.

Figure 3. Top panels show total monthly precipitation (left) and daily tide levels (right). Daily average water levels relative to NAVD88 are shown in the left-side panels and daily average specific conductivity (SC) are shown in the right-side panels for all monitoring locations. Note y-axis rescaled at 3 mS/cm for Farm B SC and at 1 mS/cm for Farm C shallow wells. Precipitation data were obtained from NOAA National Estuarine Research Reserve System for the St. Jones station, and tidal data was from the NOAA tide gauge 8537121 Ship John Shoal, NJ.

Figure 4. Water levels and SC from Farm A during the period in 2019 when Marsh A became dry while SC levels in Pond A increased, indicating flow of brackish groundwater into the pond.

Figure 5. Daily tide levels, referenced to NAVD88, and specific conductivity (SC) from all monitoring sites starting from 10 days before to 5 months after the passing of Tropical Storm Melissa. Immediate increases in SC can be seen in all surface water bodies and SW-C2. Note re-scale of y-axes on the Farm B plot at 3 mS/cm and the Farm C shallow wells plot at 1 mS/cm.

Figure 6. Schematic of water use distributions and salinization pathways. Panels (I) are simplified map views of the distribution of water users and water bodies in the Dover, Delaware area. The letters correspond to the cross-sectional panels (II) which illustrate mechanisms of SWI into the

fresh groundwater. The relative size of the green crop irrigation circles corresponds to relative pumping amounts (i.e. wells in larger circles pump more water). Black arrows represent groundwater flow direction and red arrows signify the potential movement of saltwater due to a rise in sea level caused by high tides, storm surges and/or climate change, as well as reduction in freshwater hydraulic head from increased pumping. In panel IIc, the dashed lines represent water table elevation (black) and freshwater-saltwater interface (red) under pumping conditions.

Figure 7. Groundwater withdrawals from the Columbia and Cheswold aquifers by the City of Dover during May – Oct., which coincides with irrigation by farmers, and Nov. – Dec. (data provided by Delaware Dept. of Natural Resources and Environmental Control).